RSC Advances

ROYAL SOCIETY OF CHEMISTRY

www.rsc.org/advances

Effects of L-lactide and D,L-lactide in poly(lactide-co-glycolide)-poly(ethylene glycol)-poly(lactide-co-glycolide) on the bulk states of triblock copolymers, and their thermogellation and biodegradation in water

Chang Chen[a], Lin Chen[a], Luping Cao[a], Wenjia Shen[a], Lin Yu*[,a,b] and Jiandong Ding[a,b]

[a] State key Laboratory of Molecular Engineering of Polymers, Department of Macromolecular Science, Laboratory of Advanced Materials, Fudan University, Shanghai, 200433, P. R. China

[b] Key Laboratory of Smart Drug Delivery of Ministry of Education, School of Pharmacy, Fudan University, Shanghai, 201203, P. R. China

* Corresponding author. Tel.: 086-021-65642531; fax: 086-021-65640293.

E-mail address: yu_lin@fudan.edu.cn

Abstract: Two series of poly(L-lactide-co-glycolide)-poly(ethylene glycol)-poly(L-lactide-co-glycolide) (PLLGA-PEG-PLLGA) and poly(D,L-lactide-co-glycolide)-poly(ethylene glycol)-poly(D,L-lactide-co-glycolide) (PDLLGA-PEG-PDLLGA) triblock copolymers with similar molecular weights but different ratios of lactide (LA) and glycolide (GA) were synthesized. All the PDLLGA-PEG-PDLLGA polymers were sticky pastes at dry state and their aqueous solutions underwent a sol-gel transition upon heating; while the PLLGA-PEG-PLLGA polymers presented various bulk states from sticky paste to powder and possessed different behaviors in water, which was dependent upon L-LA/GA ratio. An appropriate L-LA/GA ratio not only led to a solid-like form at the bulk state, but also formed a stable sol in water prior to thermo-induced physical gelation for the obtained polymer. This feature was convenient for weighing, transferring and storing in the potential material applications. The effects of steric regularity in PLGA block on the thermogelling and degradation of triblock copolymers in water were further examined. At high LA/GA ratio, solid-like PLLGA-PEG-PLLGA showed significant difference in both thermogellation properties and degradation behaviors compared with sticky PDLLGA-PEG-PDLLGA. Consequently, the present study sheds light on the relationship between thermogelation and polymeric molecular structure and enriches the molecular design of the thermogelling systems as injectable biomaterials, based on commonly used monomers.

Keywords: Steric regularity, poly(lactide-co-glycolide), sol-gel transition, thermogelling, biodegradation

Introduction

Hydrogels are a kind of synthetic or natural polymers which can absorb a large amount of water and meanwhile maintain their physically or chemically cross-linked three-dimensional networks.[1-6] Due to their soft-tissue-like modulus and excellent biocompatibility, hydrogels have been widely applied in biomedical fields.[7-11] Especially, in situ-forming hydrogels with a thermo-reversible sol-gel transition have been drawing increasing attention.[12-14] Such a system is a free-flowing sol at low or room temperature and spontaneously forms a semi-solid gel at the physiological temperature after being injected into the mammal body. Typical thermogelling polymers are amphiphilic with a delicate balance between hydrophilicity and hydrophobicity, consisting of poly(ethylene glycol) (PEG) and poly(D,L-lactide-co-glycolide) (PLGA),[15-17] PEG and poly(□-caprolactone) (PCL),[18-20] PEG and poly(□-caprolactone-co-D,L-lactide) (PCLA),[21-24] PEG and polypeptides,[25-27] and poly(phosphazenes).[28, 29] These resulting hydrogels as minimally invasive implants have great potentials in medicine such as drug delivery carriers,[28-30] tissue engineering scaffolds,[31, 32] and matrices of preventing postoperative tissue adhesion.[33, 34]

While both PLGA and PEG are very popular medical polymers,[35-42] the block copolymers composed of them are also of much importance. In the past decade, biodegradable and thermogelling triblock copolymer PLGA-PEG-PLGA has become one of the most popular thermogels due to its convenient synthesis, good reproducibility and controllable properties.[13, 16, 43] The critical gelation concentration

(CGC), critical gelation temperature (CGT), gel modulus and in vivo gel duration of PLGA-PEG-PLGA thermogels can be fine-tuned by molecular parameters including molecular weight (MW),[16, 17] block ratio,[16] sequence of LA and GA units in the PLGA block[44] and even end groups.[17, 45] External additives such as PEG homopolymers[16, 46, 47] or salts[16, 48] can influence their thermogelling behaviors as well. To date, their biomedical applications have involved in drug delivery,[43, 49, 50] and tissue repair.[51]

As is well known, lactic acid is a chiral molecule with two optical isomers, named as L-lactic acid and D-lactic acid.[52] To the best of our knowledge, only racemic D,L-lactide (D,L-LA) monomer was used to synthesize thermogelling PDLLGA-PEG-PDLLGA triblock copolymer so far. The obtained product is a sticky paste at the bulk state, resulting in the difficulty in handling such as weighing, transferring and dissolving.[18, 43]

Generally, stereochemistry plays an important role in adjusting and controlling the physicochemical property of material. Poly(L-lactide-co-glycolide) (PLLGA) or poly(L-lactide) (PLLA) was known to degrade more slowly than that made from racemic monomers.[36, 53, 54] The stereocomplex between PLLA-PEG-PLLA and poly(D-lactide)-poly(ethylene glycol)-poly(D-lactide) (PDLA-PEG-PDLA) in water exhibited a sol-gel transition as the temperature increased. Nevertheless, the enantiomeric counterparts were just water-soluble in a broad temperature region.[55] Thermogelling PEG/PLLA multiblock copolymer showed a wider gel window and a higher gel modulus as compared to PEG/PDLLA multiblock copolymer.[56]

In this study, we synthesized poly(L-lactide-co-glycolide)-poly(ethylene

glycol)-poly(L-lactide-co- glycolide) (PLLGA-PEG-PLLGA) triblock copolymers as well as poly(D,L-lactide-co-glycolide)-poly(ethylene glycol)-poly(D,L-lactide-co-glycolide) (PDLLGA-PEG-PDLLGA). Fig. 1 shows the chemical structures of PLLGA-PEG-PLLGA and PDLLGA-PEG-PDLLGA. The objectives of this study are: (1) to confirm that such a kind of triblock copolymers still can maintain the capacity of thermogelation in water for the first time, (2) to achieve a solid-like morphology at dry state for convenient handling in practical application, (3) to investigate the structure-property relationship of the sol-gel transition by altering steric regularity in PLLGA block, (4) to examine and compare thermogelling properties and degradation behaviors of such a thermogel versus the traditional PDLLGA-PEG-PDLLGA hydrogel.

Fig. 1

Materials and methods

Materials

PEG of MW 1500 and stannous octoate ($Sn(Oct)_2$, purity of 95%) were purchased from Aldrich and used without further purification. D,L-lactide (D,L-LA) and glycolide (GA) were products of Purac. L-lactide (L-LA) was obtained from Jinan Daigang Biomaterial Co., Ltd (China). All other reagents were of reagent grade and used in the experiments as received.

Synthesis of PLLGA-PEG-PLLGA and PDLLGA-PEG-PDLLGA triblock copolymers

Triblock copolymers with different L-LA/GA or D,L-LA/GA ratios were prepared via ring-opening copolymerization using PEG as a macromolecular initiator. The detailed synthetic procedure has been described in our previous publications.[57, 58] Briefly, PEG (10 g) was added into a 250-mL three-neck round-bottom flask and heated under vacuum (200 Pa) to remove the residual moisture in PEG at 120 °C for 3 h. Then, LA and GA with a pre-designated amount were added and heated at 100 °C for 30 min to remove the residual moisture. After the addition of stannous octoate (0.15 wt % of monomer weight), the reaction mixtures were stirred at 140 °C for 24 h under argon atmosphere. Finally, crude polymers were obtained and purified by washing in hot water (80 °C) for 4 times. Final products were obtained after freeze drying for 2 days. A series of triblock copolymers in this study were synthesized similarly.

NMR measurements

A 500-MHz proton NMR spectrometer (Bruker, DMX500 spectrometer) was used for ^{1}H NMR measurements (in $CDCl_3$) to determine the chemical composition and structure of triblock copolymers. All spectra were recorded at room temperature.

Gel permeation chromatography characterization

A gel permeation chromatography system (GPC, Agilent 1100) equipped with a differential refractometer detector was used to measure MWs and their distributions of copolymers. MWs were calculated with polystyrene (PS) standards. Tetrahydrofuran (THF) was used as eluent at a flow rate of 1 mL/min. All the measurements were carried out at 35 °C.

Differential scanning calorimeter

The thermal behaviors of triblock copolymers were characterized via a differential scanning calorimeter (DSC Q2000, TA) in the temperature ranging from -50 to 80 °C. Firstly, 5.0 mg (weighed into the Tzero pan) of the sample was heated to 80 °C under a nitrogen atmosphere to remove thermal history, then a cooling and heating rate of 10 °C /min was set to record the thermograms of triblock copolymers. The temperature was equilibrated for 5 min at the end of each step.

X-ray diffraction

The crystallization property of triblock copolymers was measured by a PANalytical X' Pert PRO diffractometer using a Cu Kα radiation source at 40 KV with 40 mA. The diffraction angle of the measurement was recorded from 5° to 50° with a scanning step of 5 °/min at room temperature.

Sol-gel transition

The sol-gel transition was determined via the test tube inverting method with 1 °C increment temperature of per step.[16] The polymers were dissolved in phosphate buffer saline (PBS) solution and stored at 4 °C. Then, each vial (2 mL) containing 0.5 mL sample with a given concentration was immersed in a water bath for 15 min at the pre-designated temperature. The sol-gel transition temperature was monitored via inverting the test tubes. In case of no visual flow in 30 s, it was regarded as the gel formation.

Rheology analysis

A stress-controlled rheometer (Malvern, Kinexus) was also used to determine the

sol-gel transition of triblock copolymer in PBS solution (25 wt %). About 1.5 mL of polymeric solution was added on the plate (diameter: 60 mm, conical degree: 1°). Then, the cone plate was lowered to a fixed height (0.03 mm gap). The edge of the sample was overlaid with a layer of low viscosity silicone oil to reduce the water evaporation. The data was collected at a frequency of 5 rad/s and an appropriate strain according to the linear viscoelastic regions. An oscillation single frequency stress test mode was first set with a trigger of stress. Once the strain was less than 1%, the oscillation single frequency stress mode would be replaced by the strain one. The heating rate was 0.5 ℃/min controlled by a plate environmental semiconductor with a temperature resolution of ±0.001 ℃. Both storage modulus $G^{'}$ and loss modulus $G^{''}$ were obtained in oscillation shear flow. The complex modulus (G^{*}) was calculated from $G^{'}$ and $G^{''}$ by the equation $G^{*} = \sqrt{G^{'2} + G^{''2}}$.

In vitro degradation

The triblock copolymer aqueous solutions (25 wt % in PBS, 0.5 mL) were added into test tubes and equilibrated at 4 ℃ overnight. Then, the samples were incubated in a shaking bath with 50 stoke/min at 37 ℃ for 10 min to form in situ hydrogels. Next, 5 mL of PBS solution (pH 7.4) was added into the tubes and buffer solutions were replaced with fresh ones at predetermined time intervals. Some samples were taken out from the shaking bath at each designated time point, and buffer solution was removed. The triblock copolymers in remaining gels were obtained by freeze-drying. A blank sample containing the same volume of PBS solution was freeze-dried and weighed to deduct the effect of salt in the residual gels. Measurements of weighing,

^{1}H NMR and GPC were performed to analyze the samples. The pH was also measured at designated time intervals before the medium was replaced.

In vivo gel formation

Sprague Dawley (SD) rats with an average weight of 250 g were anesthetized by diethyl ether, and then 0.4 mL of polymeric aqueous solution (25 wt % in normal saline solution) was subcutaneously injected into the neck of rat via a 23-gauge needle. All the procedures of animal experiments were carried out according to "Principles of Laboratory Animal Care". The animals were sacrificed after injection for 6 or 12 days, then the autopsy was carried out and the in situ-forming gel matrix was taken out from the target site to take photographs using a Canon digital camera.

Results and discussion

1. Synthesis and characterization of PLLGA-PEG-PLLGA and PDLLGA-PEG-PDLLGA triblock copolymers

The PLLGA-PEG-PLLGA triblock copolymers were synthesized by ring-opening polymerization of L-LA and GA in the present of PEG using stannous octoate as the catalyst. Fig. 2 displays the ^{1}H NMR spectrum of a PLLGA-PEG-PLLGA triblock copolymer. The proton signal peaks at 5.25 ppm (-C***H***(CH_3)COO-), 4.8 ppm (-C***H***$_2$COO-), and 3.65 ppm (-C***H***$_2$C***H***$_2$O-) were used to calculate the number-average MW and L-LA/GA molar ratio. Three PLLGA-PEG-PLLGA copolymers (abbreviated L-1, L-2, and L-3) with the similar MWs but various L-LA/GA ratios ranged from 1.0 to 5.0 were obtained after reaction at 140 °C for 24 h. Meanwhile, three PDLLGA-PEG-PDLLGA samples (abbreviated DL-1, DL-2, and DL-3) were also

synthesized in one-to-one correspondence to investigate the effects of steric regularity in PLGA chain on the reverse thermal gelation and degradation behaviors. All the samples were further measured via GPC to determine MWs and their distributions. The GPC traces of all polymers exhibited unimodal with a polydispersity index (weight-average MW over number-average MW, M_w/M_n) no more than 1.25. More detailed characterizations of these samples were listed in Table 1.

Fig. 2

Table 1

2. Thermal property of PLLGA-PEG-PLLGA triblock copolymers at the bulk state and the stability of their aqueous solutions

DSC was used to investigate the thermal characteristics of PLLGA-PEG-PLLGA triblock copolymers with different L-LA/GA ratios. All the samples were ramped up for the first heating, cooling and the second heating at a rate of 10 °C /min. Fig. 3a shows the thermograms of these samples of the cooling and the second heating run. The incorporation of GA into PLLA chain interrupted the crystallization of PLLA and PEG blocks. For L-1 and L-2, neither crystallization peak nor melting peak was observed in both cooling and heating curves, indicating that the two specimens are amorphous. In the case of L-3 with high L-LA content, the crystallization peak did not appear during the cooling curve but during the second heating curve. A similar pattern was found in PEO-PLLGA diblock copolymer and this feature arose from the partial phase mixing between PLLGA blocks and PEG blocks.[59] The crystallization peak and

the melting peak of PLLA component were detected at 32 °C and 58 °C, respectively, in the heating process. Therefore, with increasing L-LA/GA ratio, the steric regularity in PLLGA chain increased, resulting in the formation of crystallization. In addition, the glass transition temperature (T_g) of the three samples was also detected. PDLLA blocks are known to be amorphous and the incorporation GA into PDLLA block led to a more random PLGA chain. As a result, all the PDLLGA-PEG-PDLLGA triblock copolymers exhibited an amorphous state with an obvious T_g (Fig. 3a just shows the data of DL-2).

Fig. 3

The XRD measurements were also performed to confirm the crystalline or amorphous state of PLLGA-EGP-PLLGA triblock copolymers with the results shown in Fig. 3b. For L-3, two strong diffraction peaks at 16.6° and 17.7° and two weak diffraction peaks at 19.9° and 21.9° were detected, respectively. The strong peaks were ascribed to the crystal of the PLLA component,[60] while the weak peaks were attributed to the crystal of the PEG component.[35] No crystallization peak was observed and the XRD pattern just showed a broad amorphous peak for the other three samples. These results were consistent with the DSC characterizations.

Fig. 4 displays the morphology, solubility and sol stability of three PLLGA-PEG-PLLGA triblock copolymers. All the PDLLGA-PEG-PDLLGA triblock copolymers exhibited sticky morphology, whereas the specimen morphology of PLLGA-PEG-PLLGA varied from sticky paste to powder form with the increase of L-LA/GA ratio, as shown in Fig. 3a. L-1 and L-2 were soluble in water and formed

homogeneous sols at room temperature; L-3 just formed an opaque suspension liquid in water, as presented in Fig. 3b. As these samples were stored in a refrigerator at 4 ℃ for one week, L-3 was precipitated in water. In contrast, the other two samples kept a stable sol state. Fortunately, amorphous L-2 took on a solid-like form after freeze-dried. Such a product was easy to weigh and transfer compared with a paste one. Therefore, the L-LA content in PLLGA block is a crucial parameter for designing the PLLGA-PEG-PLLGA triblock copolymers with a solid-like morphology at dry state and a stable sol in water.

Fig. 4

3. Sol-Gel transition of PLLGA-PEG-PLLGA and PDLLGA-PEG-PDLLGA triblock copolymers in water

L-3 with high L-LA content was insoluble in water due to its crystallization, as shown in Fig. 4c and Table 1. Aside from L-3, other PLLGA-EPG-PLLGA and PDLLGA-PEG-PDLLGA triblock copolymers were soluble in water at low or room temperature and underwent a sol-gel transition as temperature increased. The polymer aqueous solution formed a translucent gel with raising temperature and then transformed into an opaque gel as the temperature further increased. When the thermogel was left at a low temperature (4 ℃), it turned into a clear solution again, indicating its thermoreversible property.

The phase diagrams of the two water-soluble PLLGA-PEG-PLLGA triblock copolymers are presented in Fig. 5a. Both CGC and CGT were achieved via phase

diagram. For example, the lower CGT of a 25% polymer system changed from 34 ℃ to 37 ℃ with increasing L-LA/GA ratio from 1.0 (L-1) to 1.8 (L-2). Meanwhile, the upper CGT increased from 51 ℃ to 58 ℃ as well. Interestingly, their CGCs were almost the same and the gel window widths were similar. Fig. 5b shows the phase diagrams of PLLGA-PEG-PLLGA and PDLLGA-PEG-PDLLGA triblock copolymers with a given LA/GA ratio (1.8). Sticky DL-2 showed a smaller CGC and a lower CGT compared with solid-like L-2.

Fig. 5

To further study the sol-gel transition of triblock copolymer aqueous solutions, the dynamic rheological measurements were carried out with the results displayed in Fig. 6. Following the sol-gel transition of polymeric aqueous solution, an abrupt increase in storage modulus (G') and loss modulus (G'') was observed. Fig. 6a presents the change in modulus of L-1 and L-2 as a function of temperature. Generally speaking, the crossover point between G' and G'' was defined as the sol-gel transition temperature (T_{gel}).[61, 62] The T_{gel} of L-1 was about 34 ℃, which was lower than that of L-2 (37 ℃). These findings were consistent with the results presented in Fig. 5, which were determined via the vial inverting approach. Interestingly, with elevating L-LA/GA ratio, both the T_{gel} and the maximal modulus obviously increased.

Fig. 6

We also evaluated the influence of steric regularity on the thermogelation property of PLLGA-PEG-PLLGA and PDLLGA-PEG-PDLLGA triblock copolymers. Both L-1 and DL-1 with 1.0 LA/GA ratio presented sticky pastes at the bulk state and the

rheological measurements of their aqueous solutions (25 wt %) are displayed in Fig. 6b. Not only the maximal modulus of both samples was very close but also the T_{gel} was almost the same (34 °C). This finding suggested that if the L-LA content was not dominant in PLLGA component, the change in steric regularity of PLLGA-PEG-PLLGA triblock copolymers was not enough to alter their bulk morphology and thermogelling properties compared with corresponding PDLLGA-PEG-PDLLGA triblock copolymers.

With increasing LA/GA ratio from 1.0 to 1.8, DL-2 still maintained a sticky paste form, whereas L-2 presented a solid-like morphology as a neat polymer due to the higher steric regularity. Although the maximal modulus of both samples was similar in magnitude, as shown in Fig. 6c, the difference in T_{gel} was observed. The sample L-2 read 37 °C while DL-2 read 33 °C, suggesting that high L-LA content not only influenced the morphology of copolymers at the bulk state, but also changed the T_{gel}.

The effect of heating rate on the profiles of G' and G'' in sol-gel transition was evaluated as well. Fig. 7 shows the dynamic rheological measurements of DL-2 and L-2 aqueous solutions (25 wt %) with varying the heating rate from 0.2 °C /min to 1.0 °C /min. No significant difference was observed in modulus and T_{gel} for both samples. Therefore, the heating rate did not affect the gelation property of these copolymers with different steric regularity in rheological measurements.

Fig. 7

4. In vitro degradation

Biodegradability is vital for biomaterials. The degradation of PLGA-PEG-PLGA hydrogel mainly depends on the hydrolysis of PLGA segments.[63] Generally, the high GA content resulted in the fast hydrolysis rate.[64, 65] In this study, we examined the influence of steric regularity in hydrophobic polyester block on the degradation of PLLGA-PEG-PLLGA and PDLLGA-PEG-PDLLGA hydrogels. Considering that no significant difference between L-1 and DL-1 was observed, we focused on the other two samples. Fig. 8 shows the photographs of L-2 and DL-2 thermogels at given time points in PBS at 37 °C. L-2 thermogel showed a translucent state at the body temperature before degradation, while DL-2 was an opaque state at the same condition. L-2 thermogel gradually swelled at the initial stage of degradation and then presented an oppositely contractive trend at the late stage. DL-2 hydrogel also exhibited a swelling tendency at the initial stage. At the 14th day, its disintegration of gel occurred and a significant amount of water-soluble products were dissolved into the buffer system (see the dashed ellipse in Fig. 8b (14 D)). Afterwards, the residual substance of DL-2 continuously swelled.

Fig. 8

The remaining gels were taken out and freeze-dried to obtain the dried copolymers. The residual samples were weighed to analyze the mass loss during in vitro degradation, as shown in Fig. 9a. L-2 thermogel showed a gradual weight decrease and only about 50% mass loss occurred within a month in vitro degradation. In contrast, the polymer gel of DL-2 exhibited a trans-S-shape profile of mass loss and almost 90% mass was lost during the same degradation period. These results were

basically consistent with the visual observations in Fig. 8.

Fig. 9

The time-dependent profiles of MW of the two samples during degradation are shown in Fig. 9b. The number-average and weight-average MWs were calculated by GPC profiles using PS as standards. Both samples exhibited a steady decrease of MW during degradation and half of MW was lost after incubation in buffer solution for one month. Compared with DL-2 thermogel, the slower degradation rate was found in the L-2 one. The feature was attributed to the strong steric regularity in L-2 thermogel, resulting in the relatively less accessibility of water to the ester bonds of L-LA-rich segment. A similar pattern was found between PLLGA and PLGA polymers.[36, 53]

The change of medium pH was also recorded at each predetermined time point with the results shown in Fig. 9c. The pH value of medium of the two thermogels gradually decreased during the total experiment period even if the buffer solution was replaced at regular intervals. This finding was attributed to the hydrolysis of ester bond in PLLGA and PDLLGA blocks, resulting in the generation of lactic acid, glycolic acid and ester oligomers.[63, 64] Moreover, no significant difference was observed between the two specimens within the initial 14 days of degradation. Compared with L-2, the medium pH of DL-2 gel presented a slower change pattern at the late stage. This feature resulted from the disintegration of DL-2 at the 14^{th} day (Fig. 9b). Due to a large amount of mass loss during its disintegration, the residual DL-2 could not generate the same amount of acidic products of degradation as L-2 during the same period.

Fig. 10 presents some typical GPC profiles for the two samples in the examined period of degradation. The GPC profiles of the two copolymers took on a unimodal distribution before degradation. A slow increase of retention time at peak maximum was observed during in vitro degradation, indicating a gradual decrease of MW for the two copolymers. The single-peak profile was maintained during the degradation period of one month for DL-2 copolymer. However, the GPC profile of L-2 turned into a multimodal distribution after degradation for 18 days. Meanwhile, the hydrolysis rate of L-2 was found to be lower than that of DL-2, which was consistent with the results shown in Fig. 9b.

Fig. 10

The composition change of remaining copolymers was further analyzed by ^{1}H NMR. All the samples were extracted by the solvent $CDCl_3$ and then measured under the same condition to reduce the experimental errors. Fig. 11a shows change in ^{1}H NMR spectra of the two copolymers before degradation and after 30 days degradation in PBS at 37 °C. Similar to a previous report,[63] the height of methyl peak of PLLGA or PDLLGA block at 5.25 ppm significantly increased after degradation. The fractions of LA, GA, and EG were determined via calculation of the integrated areas at 5.25, 4.8, and 3.65 ppm in the ^{1}H NMR spectra. Both copolymers displayed a similar pattern of composition change in the examined periods of degradation (Fig. 11b). The EG fraction gradually decreased while the LA fraction increased during degradation. On one hand, this feature suggested a preferential mass loss of PEG-rich segments. On the other hand, the result provided evidence of the hydrolytic degradation of

polyester chain, which also has been demonstrated via GPC measurements. Interestingly, the GA fraction slightly changed at the same period of degradation. It is well-known that GA could preferentially connect to PEG during the ring-opening polymerization due to its higher reactivity than LA and the obtained GA segment presented the faster rate of chain scission compared with LA segment.[64] As a result, some GA might be diffused into the buffer solution along with PEG during degradation, resulting in counteracting the increase of PDLLGA or PLLGA segment.

Fig. 11

5. In vivo gel formation and degradation

To investigate the influence of steric regularity on in vivo degradation, L-2 and DL-2 copolymer aqueous solutions were subcutaneously injected into the neck of SD rats, respectively. An obvious elliptic protrusion appeared at the target site, reflecting the formation of in-situ gel. After 6 and 12 days, the animals were sacrificed and the gel matrices were taken out from the injection site with the results shown in Fig. 12. No significant difference in size was observed 6 days after injection. At the 12^{th} day, both specimens became strikingly smaller than those at the 6^{th} day. Meanwhile, compared with L-2 gel with globular shape, flat DL-2 thermogel presented a preferential mass loss, indicating the faster degradation rate of DL-2 gel during in vivo test. This finding was consistent with the in vitro results.

Fig. 12

Conclusions

It is the first report on the thermogelling PLLGA-PEG-PLLGA systems. PLLGA-PEG-PLLGA and PDLLGA-PEG-PDLLGA triblock copolymers with similar MWs but various monomer ratios were synthesized and characterized. Although the sticky morphology of PDLLGA-PEG-PDLLGA at the bulk state was independent of D,L-LA/GA ratio, the different forms of PLLGA-PEG-PLLGA from sticky paste to powder were achieved by varying L-LA/GA ratio to adjust the steric regularity of PLLGA chain. An expected PLLGA-PEG-PLLGA polymer with a solid-like form at dry state was obtained, which was able to form a stable sol in water at room temperature and transform into a non-flowing gel in response to an increase in temperature. The solid-like morphology was convenient for practical application such as weighing, transferring, and storing.

At the LA/GA ratio of 1.0, PLLGA-PEG-PLLGA and PDLLGA-PEG-PDLLGA not only presented the same sticky morphology, but also underwent the similar sol-gel transition upon heating. PLLGA-PEG-PLLGA maintained a sticky form at dry state as the L-LA/GA ratio increased to 1.5 (data not shown). With further increasing the LA/GA ratio to 1.8, solid-like PLLGA-PEG-PLLGA was achieved. It showed a similar gel modulus but a higher sol-gel transition temperature and a slower degradation rate compared with the correspondingly sticky PDLLGA-PEG-PDLLGA. This difference was attributed to the influence of steric regularity in the hydrophobic polyester chain. It is worth pointing out that the thermogelling regions of the L samples were relatively narrow compared with the D,L ones. Hence, the current study

gives more insight in the molecular design of the underlying thermogelling polymers as injectable hydrogels and provides beneficial molecular parameters for corresponding polyether/polyester block copolymers.

Acknowledgment

The group was supported by NSF of China (Grants No. 51273217, No. 91127028, and No. 21034002), Chinese Ministry of Science and Technology (973 Program No. 2011CB606203) and Science and Technology Developing Foundation of Shanghai (Grants No. 12JC1402600 and No. 13XD1401000).

References

1. N. A. Peppas, P. Bures, W. Leobandung and H. Ichikawa, *Eur. J. Pharm. Biopharm.*, 2000, **50**, 27-46.
2. E. A. Appel, J. del Barrio, X. J. Loh and O. A. Scherman, *Chem. Soc. Rev.*, 2012, **41**, 6195-6214.
3. S. Tungchaiwattana, R. Liu, S. Halacheva, N. N. Shahidan, A. Kells and B. R. Saunders, *Soft Matter*, 2013, **9**, 3547-3557.
4. T. L. Sun, T. Kurokawa, S. Kuroda, A. B. Ihsan, T. Akasaki, K. Sato, M. A. Haque, T. Nakajima and J. P. Gong, *Nat. Mater.*, 2013, **12**, 932-937.
5. A. Sanchez-Ferrer, V. K. Kotharangannagari, J. Ruokolainen and R. Mezzenga, *Soft Matter*, 2013, **9**, 4304-4311.
6. J. Wu, Q. Zhao, C. Liang and T. Xie, *Soft Matter*, 2013, **9**, 11136-11142.
7. B. Jeong, Y. H. Bae, D. S. Lee and S. W. Kim, *Nature*, 1997, **388**, 860-862.
8. A. S. Hoffman, *Adv. Drug Deliv. Rev.*, 2002, **54**, 3-12.
9. T. Vermonden, R. Censi and W. E. Hennink, *Chem. Rev.*, 2012, **112**, 2853-2888.
10. F. Chicatun, N. Muja, V. Serpooshan, T. M. Quinn and S. N. Nazhat, *Soft Matter*, 2013, **9**, 10811-10821.
11. Y. P. Fan, C. Deng, R. Cheng, F. H. Meng and Z. Y. Zhong, *Biomacromolecules*, 2013, **14**, 2814-2821.
12. C. L. He, S. W. Kim and D. S. Lee, *J. Control. Release*, 2008, **127**, 189-207.
13. L. Yu and J. D. Ding, *Chem. Soc. Rev.*, 2008, **37**, 1473-1481.
14. H. J. Moon, D. Y. Ko, M. H. Park, M. K. Joo and B. Jeong, *Chem. Soc. Rev.*, 2012, **41**, 4860-4883.

15. B. Jeong, Y. H. Bae and S. W. Kim, *Macromolecules*, 1999, **32**, 7064-7069.
16. M. S. Shim, H. T. Lee, W. S. Shim, I. Park, H. Lee, T. Chang, S. W. Kim and D. S. Lee, *J. Biomed. Mater. Res. Part A*, 2002, **61**, 188-196.
17. L. Yu, G. Chang, H. Zhang and J. Ding, *J. Polym. Sci., Part A: Polym. Chem.*, 2007, **45**, 1122-1133.
18. S. J. Bae, J. M. Suh, Y. S. Sohn, Y. H. Bae, S. W. Kim and B. Jeong, *Macromolecules*, 2005, **38**, 5260-5265.
19. D. Y. Kim, D. Y. Kwon, B. N. Lee, H. W. Seo, J. S. Kwon, B. Lee, D. K. Han, J. H. Kim, B. H. Min, K. Park and M. S. Kim, *Soft Matter*, 2012, **8**, 7638-7648.
20. W. W. Wang, L. L. Chang, X. Li, Y. L. Wu, J. F. Xing, L. D. Deng and A. J. Dong, *Soft Matter*, 2012, **8**, 1575-1583.
21. Z. Q. Jiang, X. M. Deng and J. Y. Hao, *J. Polym. Sci., Part A: Polym. Chem.*, 2007, **45**, 4091-4099.
22. Z. Zhang, Y. Lai, L. Yu and J. Ding, *Biomaterials*, 2010, **31**, 7873-7882.
23. A. Petit, B. Muller, P. Bruin, R. Meyboom, M. Piest, L. M. J. Kroon-Batenburg, L. G. J. de Leede, W. E. Hennink and T. Vermonden, *Acta Biomater.*, 2012, **8**, 4260-4267.
24. A. Petit, B. Müller, R. Meijboom, P. Bruin, F. van de Manakker, M. Versluijs-Helder, L. G. J. de Leede, A. Doornbos, M. Landin, W. E. Hennink and T. Vermonden, *Biomacromolecules*, 2013, **14**, 3172-3182.
25. M. K. Nguyen, D. K. Park and D. S. Lee, *Biomacromolecules*, 2009, **10**, 728-731.
26. E. Y. Kang, B. Yeon, H. J. Moon and B. Jeong, *Macromolecules*, 2012, **45**, 2007-2013.
27. Y. L. Cheng, C. L. He, C. S. Xiao, J. X. Ding, H. T. Cui, X. L. Zhuang and X. S. Chen, *Biomacromolecules*, 2013, **14**, 468-475.
28. J. K. Cho, C. Chun, H. J. Kuh and S. C. Song, *Eur. J. Pharm. Biopharm.*, 2012, **81**, 582-590.
29. J. I. Kim, B. S. Lee, C. Chun, J. K. Cho, S. Y. Kim and S. C. Song, *Biomaterials*, 2012, **33**, 2251-2259.
30. G. T. Chang, T. Y. Ci, L. Yu and J. D. Ding, *J. Control. Release*, 2011, **156**, 21-27.
31. K. Nagahama, T. Ouchi and Y. Ohya, *Adv. Funct. Mater.*, 2008, **18**, 1220-1231.
32. H. K. Kim, W. S. Shim, S. E. Kim, K. H. Lee, E. Kang, J. H. Kim, K. Kim, I. C. Kwon and D. S. Lee, *Tissue Eng. Part A*, 2009, **15**, 923-933.
33. Z. Zhang, J. Ni, L. Chen, L. Yu, J. W. Xu and J. D. Ding, *Biomaterials*, 2011, **32**, 4725-4736.
34. Z. Zhang, J. Ni, L. Chen, L. Yu, J. W. Xu and J. D. Ding, *J. Biomed. Mater. Res. Part B*, 2012, **100B**, 1599-1609.
35. H. Bley, B. Fussnegger and R. Bodmeier, *Int. J. Pharm.*, 2010, **390**, 165-173.
36. J. Li, R. M. Stayshich and T. Y. Meyer, *J. Am. Chem. Soc.*, 2011, **133**, 6910-6913.
37. Y. He, Z. Pan and J. D. Ding, *Acta Polym. Sin.*, 2013, 755-764.
38. D. X. Wang, Y. He, L. Bi, Z. H. Qu, J. W. Zou, Z. Pan, J. J. Fan, L. Chen, X. Dong, X. N. Liu, G. X. Pei and J. D. Ding, *Int. J. Nanomed.*, 2013, **8**, 1855-1865.
39. X. Wang, C. Yan, K. Ye, Y. He, Z. H. Li and J. D. Ding, *Biomaterials*, 2013, **34**, 2865-2874.
40. X. Yao, Y. Hu, B. Cao, R. Peng and J. Ding, *Biomaterials*, 2013, **34**, 9001-9009.
41. T. Y. Ci, T. Li, G. T. Chang, L. Yu and J. D. Ding, *J. Control. Release*, 2013, **169**, 329-335.
42. X. Yao, R. Peng and J. Ding, *Adv. Mater.*, 2013, **25**, 5257-5286.
43. G. M. Zentner, R. Rathi, C. Shih, J. C. McRea, M. H. Seo, H. Oh, B. G. Rhee, J. Mestecky, Z. Moldoveanu, M. Morgan and S. Weitman, *J. Control. Release*, 2001, **72**, 203-215.

44. L. Yu, Z. Zhang and J. D. Ding, *Biomacromolecules*, 2011, **12**, 1290-1297.
45. L. Yu, H. Zhang and J. D. Ding, *Angew. Chem., Int. Edit.*, 2006, **45**, 2232-2235.
46. H. Zhang, L. Yu and J. D. Ding, *Macromolecules*, 2008, **41**, 6493-6499.
47. L. Yu, G. T. Chang, H. Zhang and J. D. Ding, *Int. J. Pharm.*, 2008, **348**, 95-106.
48. T. Li, T. Y. Ci, L. Chen, L. Yu and J. D. Ding, *Polym. Chem.*, 2014, 5, 979 - 991.
49. K. Li, L. Yu, X. J. Liu, C. Chen, Q. H. Chen and J. D. Ding, *Biomaterials*, 2013, **34**, 2834-2842.
50. L. Yu, K. Li, X. J. Liu, C. Chen, Y. C. Bao, T. Y. Ci, Q. H. Chen and J. D. Ding, *J. Pharm. Sci.*, 2013, **102**, 4140-4149.
51. C. Pratoomsoot, H. Tanioka, K. Hori, S. Kawasaki, S. Kinoshita, P. J. Tighe, H. Dua, K. M. Shakesheff and F. Rose, *Biomaterials*, 2008, **29**, 272-281.
52. Y. He, W. R. Wang and J. D. Ding, *Chin. Sci. Bull.*, 2013, **58**, 2404-2411.
53. J. Li, S. N. Rothstein, S. R. Little, H. M. Edenborn and T. Y. Meyer, *J. Am. Chem. Soc.*, 2012, **134**, 16352-16359.
54. Z. Pan and J. D. Ding, *Interface Focus*, 2012, **2**, 366-377.
55. T. Fujiwara, T. Mukose, T. Yamaoka, H. Yamane, S. Sakurai and Y. Kimura, *Macromol. Biosci.*, 2001, **1**, 204-208.
56. M. K. Joo, Y. S. Sohn and B. Jeong, *Macromolecules*, 2007, **40**, 5111-5115.
57. L. Yu, Z. Zhang, H. Zhang and J. D. Ding, *Biomacromolecules*, 2009, **10**, 1547-1553.
58. L. Yu, Z. Zhang and J. D. Ding, *Macromol. Res.*, 2012, **20**, 234-243.
59. S. W. Choi, S. Y. Choi, B. Jeong, S. W. Kim and D. S. Lee, *J. Polym. Sci., Part A: Polym. Chem.*, 1999, **37**, 2207-2218.
60. N. Zhao, L. S. Wang, D. L. Huang, T. Y. Zhang, L. F. Zhang and C. D. Xiong, *Cryst. Res. Technol.*, 2010, **45**, 275-280.
61. Y. Lee, H. J. Chung, S. Yeo, C. H. Ahn, H. Lee, P. B. Messersmith and T. G. Park, *Soft Matter*, 2010, **6**, 977-983.
62. H. Zhang and J. D. Ding, *J. Biomater. Sci. Polym. Ed.*, 2010, **21**, 253-269.
63. L. Yu, Z. Zhang, H. Zhang and J. D. Ding, *Biomacromolecules*, 2010, **11**, 2169-2178.
64. M. L. T. Zweers, G. H. M. Engbers, D. W. Grijpma and J. Feijen, *J. Control. Release*, 2004, **100**, 347-356.
65. L. B. Wu and J. D. Ding, *Biomaterials*, 2004, **25**, 5821-5830.

Figure captions

Fig. 1 Chemical structures of PLLGA-PEG-PLLGA and PDLLGA-PEG-PDLLGA triblock copolymers.

Fig. 2 ^{1}H NMR spectrum of a PLLGA-PEG-PLLGA triblock copolymer (L-1) in $CDCl_3$.

Fig. 3 (a) DSC thermograms of the indicated triblock copolymers of the cooling and the second heating run. The heating and cooling rates were 10 °C /min, (b) XRD of the indicated triblock copolymers.

Fig. 4 Photographs of PLLGA-PEG-PLLGA triblock copolymers at the bulk state or in water. (a) Bulk states of L-1, L-2, and L-3; (b) sol states soon after dissolving the copolymers in water (25 wt %); (c) L-1, L-2, and L-3 aqueous solutions at 4 °C for one week in order to examine stability. Among those three polymers, only L-2 exhibited a solid-like morphology at dry state and kept a stable sol in water.

Fig. 5 Phase diagrams of PLLGA-PEG-PLLGA and PDLLGA-PEG-PDLLGA triblock copolymers in PBS with the indicated LA/GA ratios.

Fig. 6 Storage modulus G' and loss modulus G'' of the indicated samples in PBS (25 wt %) as a function of temperature. (a) L-1 and L-2; (b) L-1 and DL-1; (c) L-2 and DL-2. Heating rate: 0.5 °C /min; oscillatory frequency (ω): 5 rad/s.

Fig. 7 Influence of heating rate on G^* of the indicated copolymer aqueous solutions. Oscillatory frequency (ω): 5 rad/s.

Fig. 8 Optical images of PLLGA-PEG-PLLGA and PDLLGA-PEG-PDLLGA hydrogels at the indicated degradation intervals in PBS at 37 °C. Sample: (a) L-2, (b) DL-2. The initial polymer concentration was 25 wt %.

Fig. 9 Mass of remaining thermogels (a), number-average and weight-average MWs of copolymers in the remaining thermogels (b), pH change of the medium (c) of the indicated two samples during degradation in PBS at 37 °C. The initial polymer concentration was 25 wt %. The medium was replaced with fresh ones at regular intervals. The lines were used just for the guides of the eyes.

Fig. 10 GPC traces of the indicated two triblock copolymers before and after the given degradation period in vitro.

Fig. 11 (a) Change in ^{1}H NMR spectra during degradation of the two copolymers (L-2 and DL-2) in $CDCl_3$; (b) copolymer composition in the remaining hydrogels versus degradation time. $n = 3$ for each group.

Fig. 12 In vivo gel degradation. Images were taken at the given time after subcutaneous injection of copolymer aqueous solutions (25 wt %) into the neck of SD

rats.

Table 1. Parameters of PLLGA-PEG-PLLGA and PDLLGA-PEG-PDLLGA triblock copolymers in this study

Sample ID	Block Length[a]	LA/GA[a] (mol/mol)	M_n[b]	M_w/M_n[b]	Morphology	Solution Stability[c]
L-1	1735-1500-1735	L-LA/GA=1.0	6450	1.24	Sticky paste	Yes
L-2	1750-1500-1750	L-LA/GA=1.8	6700	1.25	Blocky solid	Yes
L-3	1670-1500-1670	L-LA/GA=5.0	6800	1.24	Powder	No
DL-1	1780-1500-1780	D,L-LA/GA=1.0	6650	1.21	Sticky paste	Yes
DL-2	1745-1500-1745	D,L-LA/GA=1.8	6400	1.21	Sticky paste	Yes
DL-3	1750-1500-1750	D,L-LA/GA=5.0	6950	1.23	Sticky paste	Yes

[a] PEG number-average M_n was provided by Aldrich, block length of PLGA and molar ratio of LA/GA were determined by ^{1}H NMR; [b] Determined by GPC; [c] Stability of solution means that copolymer aqueous solutions do not be precipitated in water or form a gel with time at room temperature.

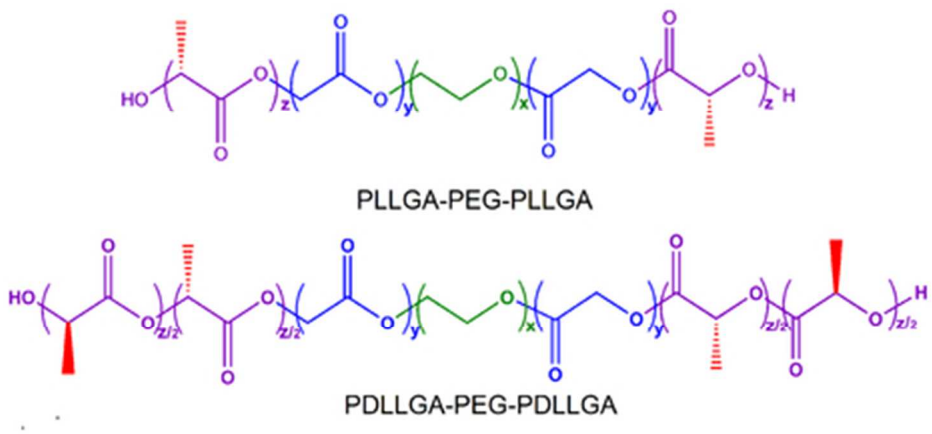

39x18mm (300 x 300 DPI)

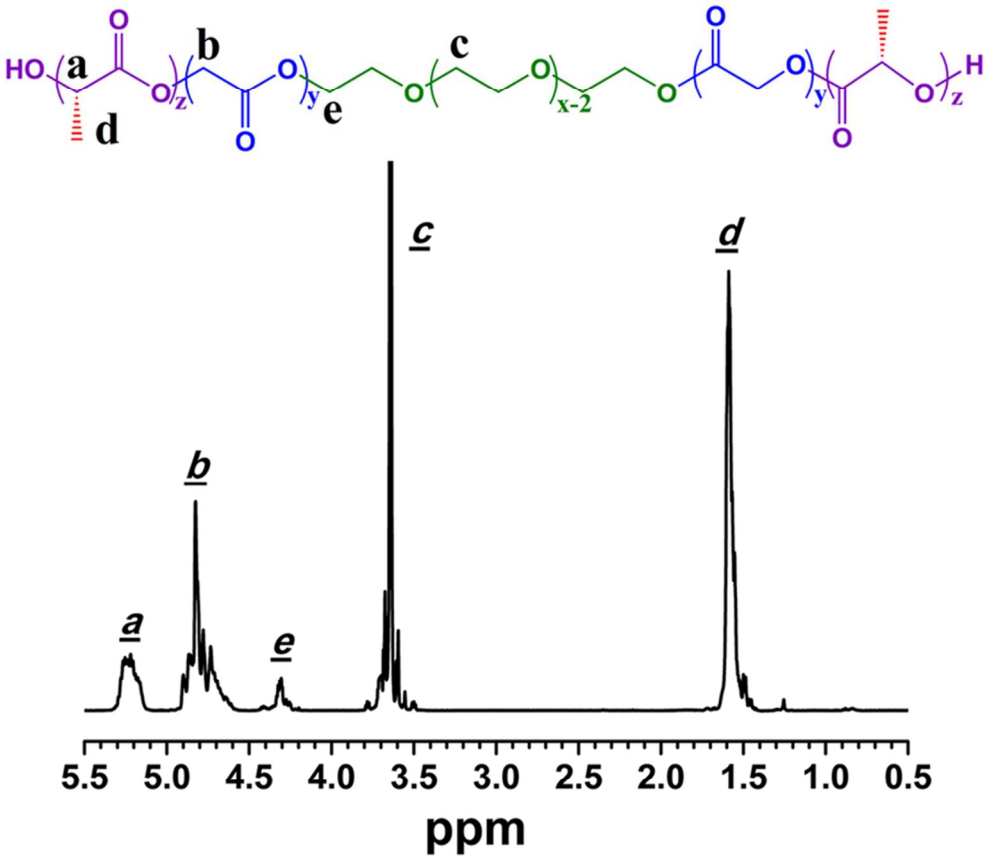

76x67mm (300 x 300 DPI)

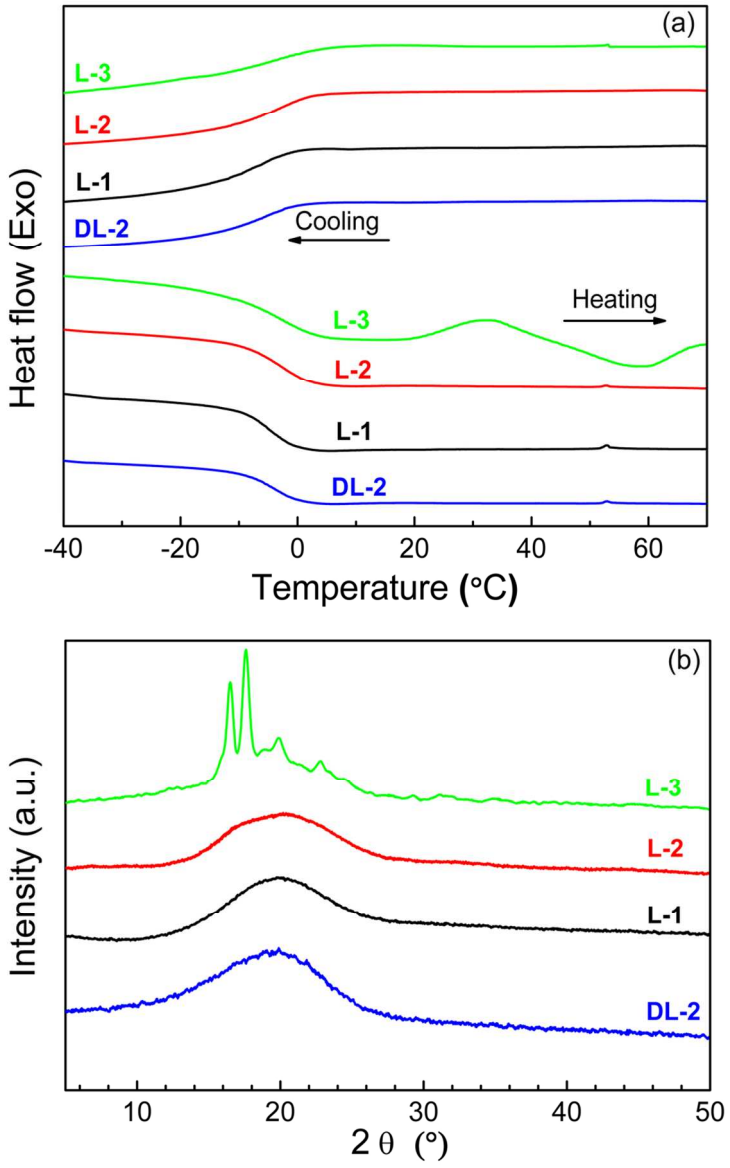

139x225mm (300 x 300 DPI)

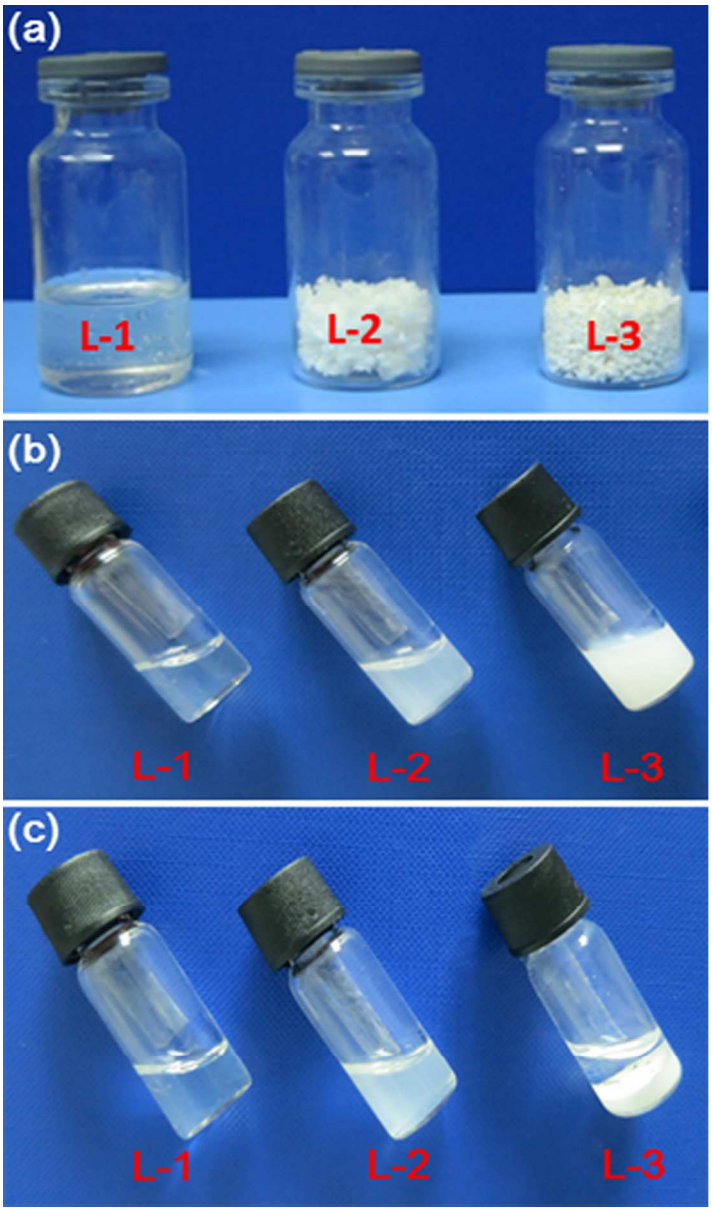

144x246mm (300 x 300 DPI)

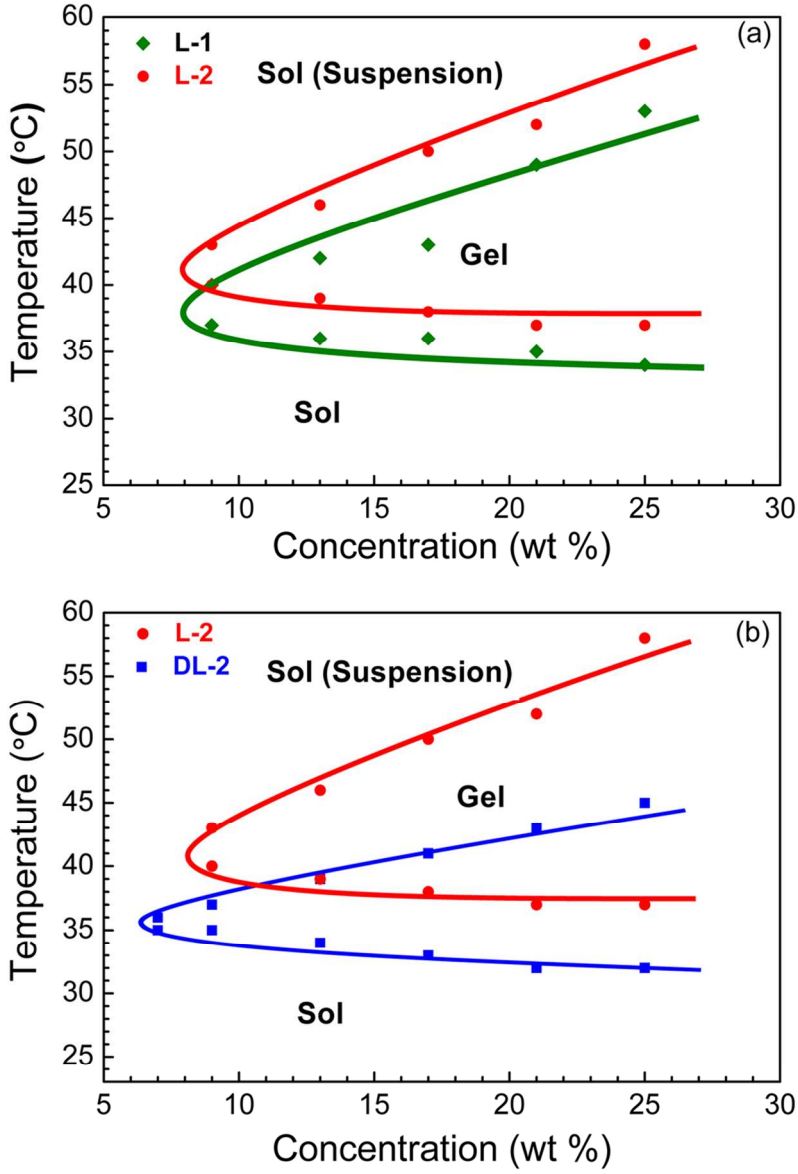

127x187mm (300 x 300 DPI)

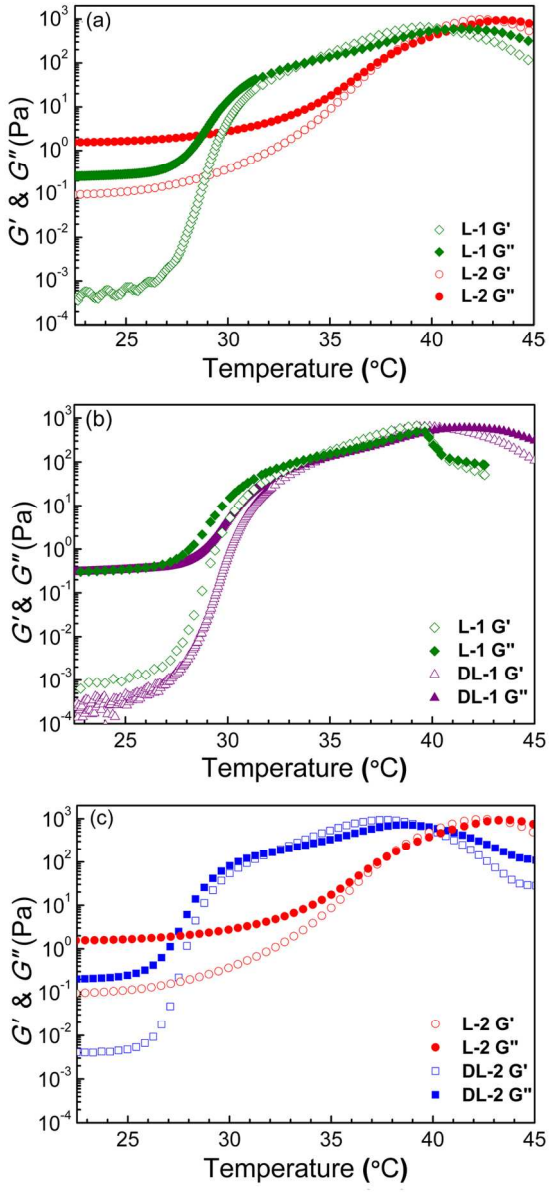

189x410mm (300 x 300 DPI)

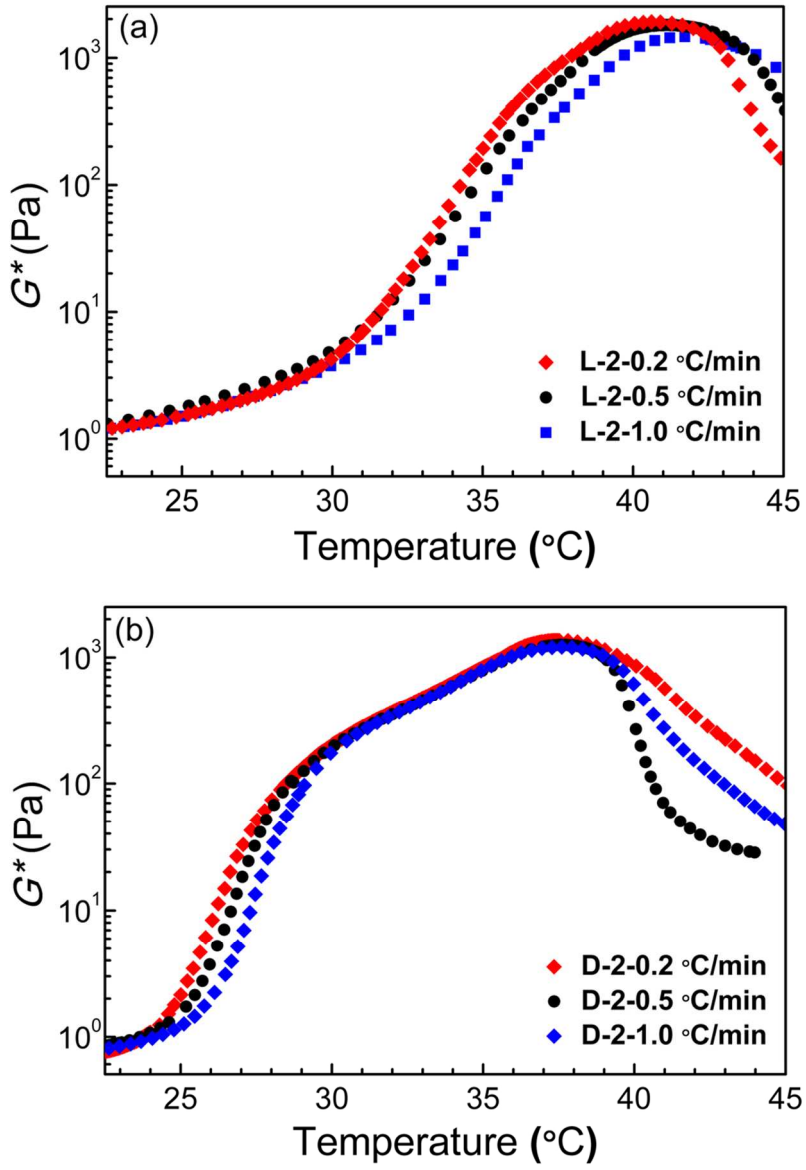

127x185mm (300 x 300 DPI)

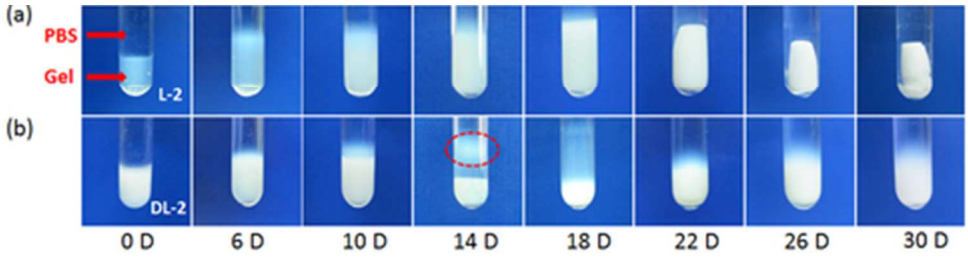

40x10mm (300 x 300 DPI)

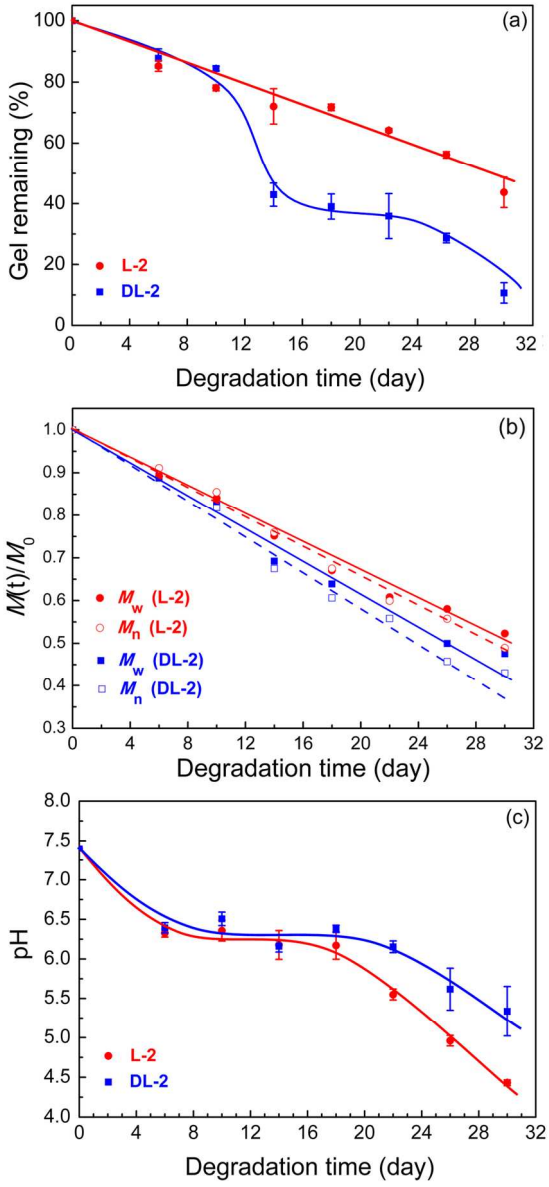

189x410mm (300 x 300 DPI)

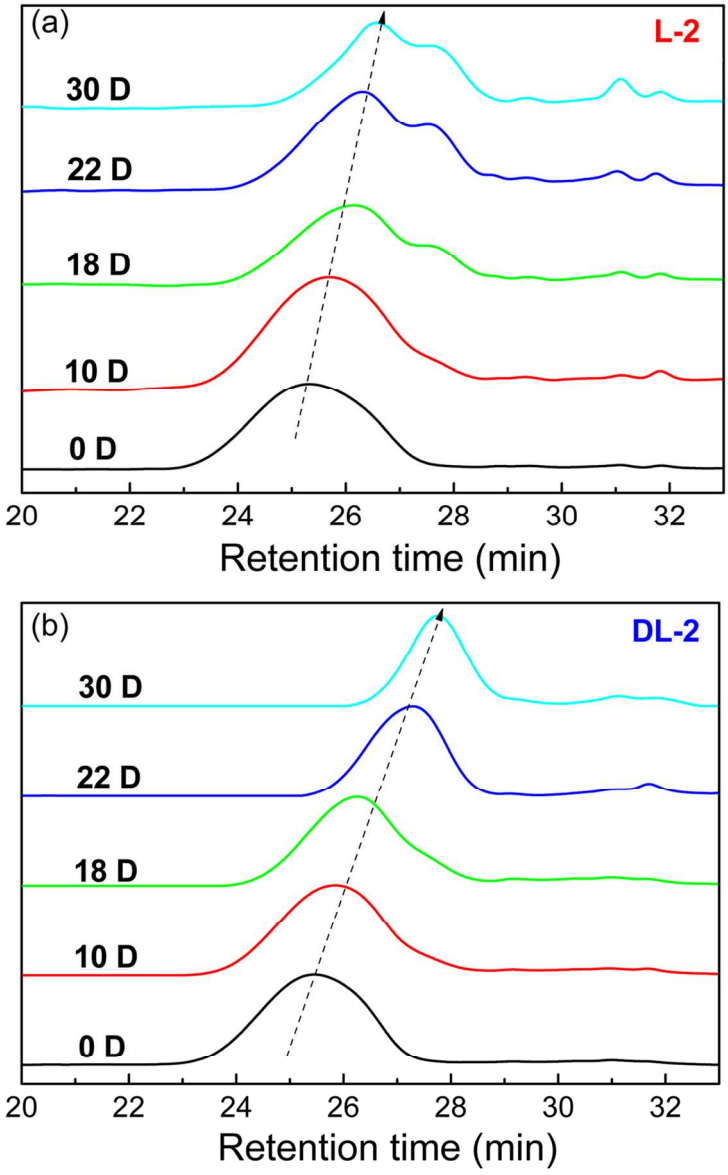

137x216mm (300 x 300 DPI)

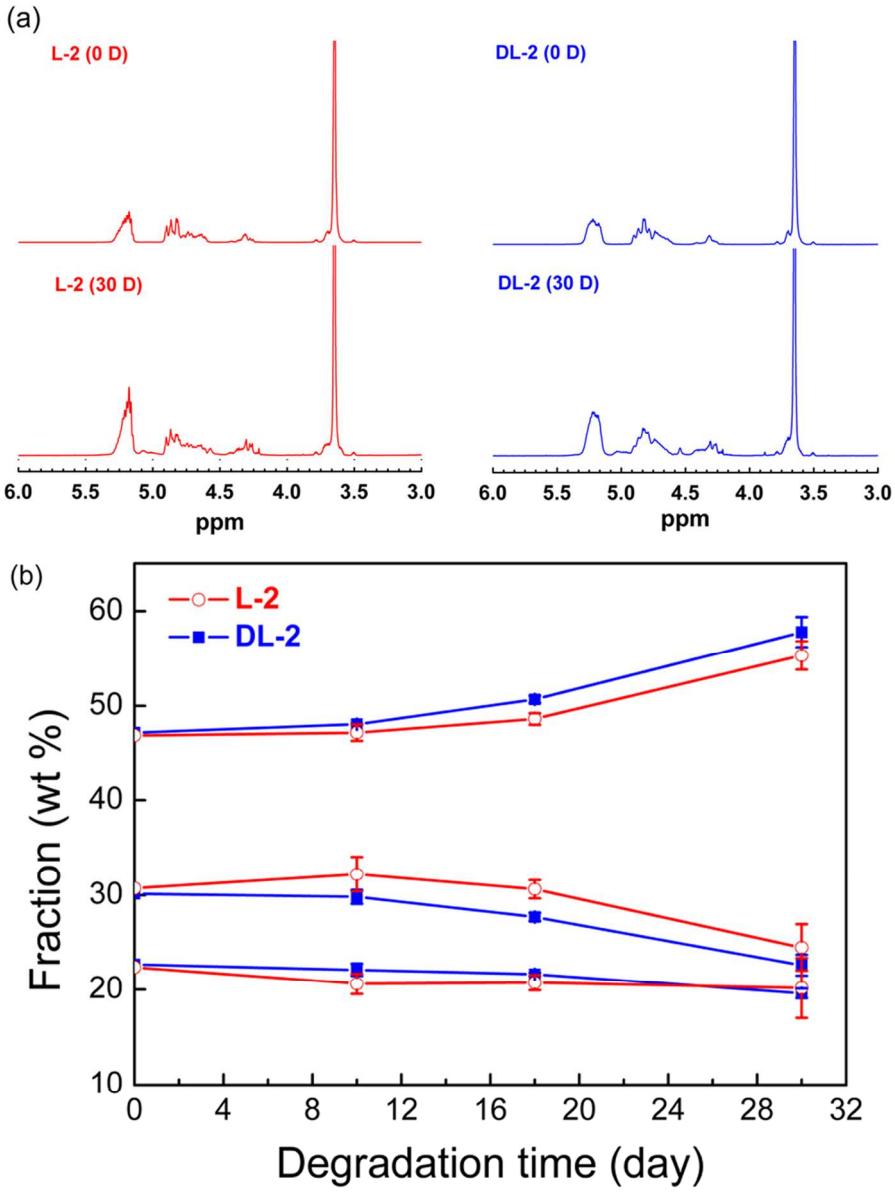

114x151mm (300 x 300 DPI)

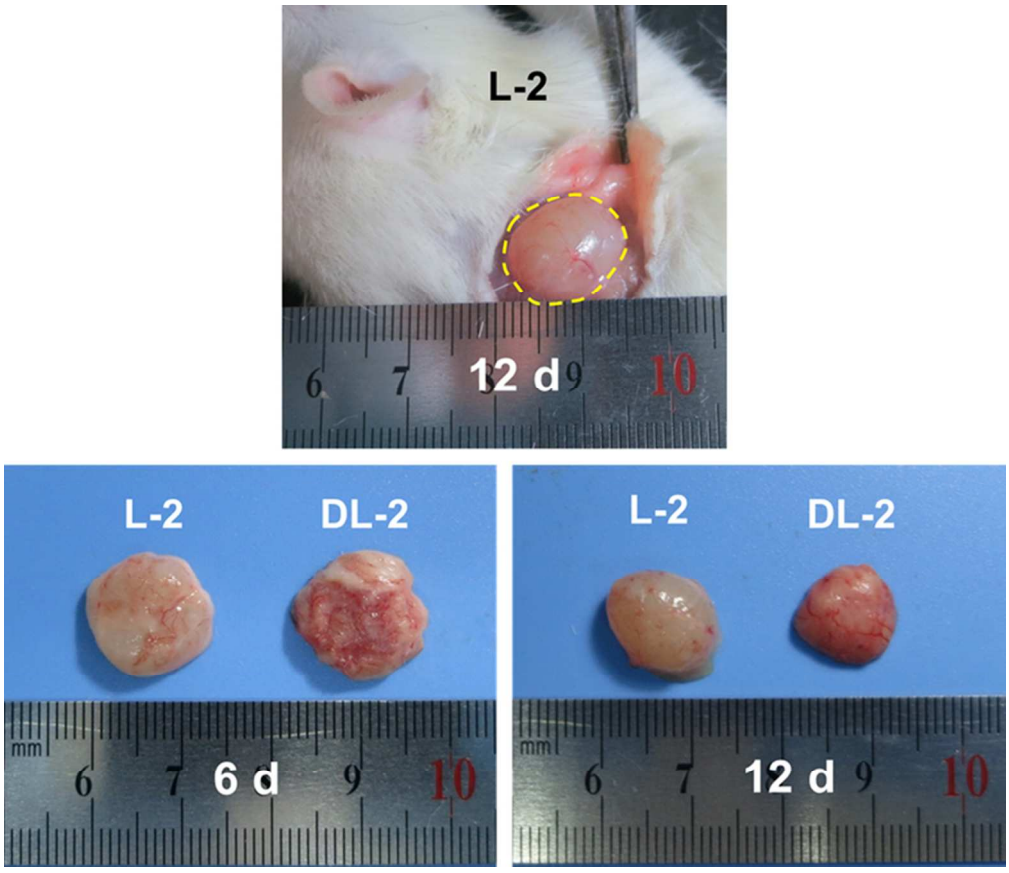

77x66mm (300 x 300 DPI)

Effects of L-lactide and D,L-lactide in poly(lactide-co-glycolide)-poly(ethylene glycol)-poly(lactide-co-glycolide) on the bulk states of triblock copolymers, and their thermogellation and biodegradation in water

Chang Chen, Lin Chen, Luping Cao, Wenjia Shen, Lin Yu* and Jiandong Ding

In this study, the effects of L-lactide and D,L-lactide on the thermogelling and biodegradation behaviors of PLGA-PEG-PLGA copolymers were revealed.